

# Superconductivity at 52 K in hole-doped C<sub>60</sub>

J. H. Schön, Ch. Kloc & B. Batlogg

Bell Laboratories, Lucent Technologies, Murray Hill, New Jersey 07974, USA

**Superconductivity in electron-doped C<sub>60</sub> was first observed almost ten years ago. The metallic state and superconductivity result from the transfer of electrons from alkaline or alkaline-earth ions to the C<sub>60</sub> molecule, which is known to be a strong electron acceptor. For this reason, it is very difficult to remove electrons from C<sub>60</sub>—yet one might expect to see superconductivity at higher temperatures in hole-doped than in electron-doped C<sub>60</sub>, because of the higher density of electronic states in the valence band than in the conduction band. We have used the technique of gate-induced doping in a field-effect transistor configuration to introduce significant densities of holes into C<sub>60</sub>. We observe superconductivity over an extended range of hole density, with a smoothly varying transition temperature  $T_c$  that peaks at 52 K. By comparison with the well established dependence of  $T_c$  on the lattice parameter in electron-doped C<sub>60</sub>, we anticipate that  $T_c$  values significantly in excess of 100 K should be achievable in a suitably expanded, hole-doped C<sub>60</sub> lattice.**

Superconductivity at relatively high temperatures in metallic C<sub>60</sub> has its origin essentially in two favourable materials properties. First, the frequency spectrum of the C<sub>60</sub> intramolecular vibrations extends to high energies ( $\sim 200$  meV) and several of these vibrations couple significantly to the electronic states, providing intramolecular electron–phonon interaction<sup>1–5</sup>. Second, the electronic density of states in the crystal is high because the weak overlap of electronic wavefunctions in the (van der Waals bonded) C<sub>60</sub> crystals leads to narrow bands. The widths of both the valence and the conduction bands are calculated to be approximately the same ( $\sim 0.5$  eV; refs 6, 7); however, the valence-band density of states (DOS) is higher<sup>6</sup> as it is derived from a fivefold degenerate ( $h_{1u}$ ) HOMO (highest occupied molecular orbital) state compared to the threefold degenerate ( $t_{1u}$ ) LUMO (lowest unoccupied molecular orbital) state. Assuming similar or slightly stronger electron–phonon coupling in the valence band (ref. 8; general reasons for enhanced  $T_c$  in hole-doped metals have been suggested in ref. 9), we thus expect a higher  $T_c$  when holes are introduced into this band. But it is very difficult to oxidize C<sub>60</sub> (refs 10, 11), and we are not aware of a successful method of producing metallic bulk C<sub>60</sub> doped with holes. (However, we note that when a fullerene mixture was exposed to highly oxidizing interhalogen vapour, magnetic signatures developed ( $\sim 50$  p.p.m. of the expected full Meissner signal) that were interpreted as being due to superconductivity in a very small portion of the sample<sup>12</sup>.)

A further question concerning the metallic state in C<sub>60</sub> can be addressed by our experiments on gate-induced doping using a field-effect transistor (FET) configuration<sup>13,14</sup> (see Fig. 1 inset): will correlation among electrons lead to a Mott–Hubbard insulating state for particular carrier concentrations? When electrons are doped into C<sub>60</sub> by chemical means, the metallic state appears to be realized for specific numbers of dopant atoms per C<sub>60</sub> molecule. In particular, the A<sub>3</sub>C<sub>60</sub> composition is the most favourable for superconductivity, while A<sub>4</sub>C<sub>60</sub> appears not even to be metallic<sup>15</sup>. The electronic structure of doped C<sub>60</sub> is therefore under discussion<sup>16,17</sup>. It is thus of fundamental interest to follow the electronic state while the doping level is continuously varied by means of the applied gate voltage, without the crystallographic changes that are inevitable when dopant atoms are incorporated into the C<sub>60</sub> lattice.

We report here our observations of gate-induced superconductivity in hole- and electron-doped C<sub>60</sub> single-crystal field-effect transistor structures. We have been able to sweep the charge carrier

density continuously from  $\sim 4.5$  holes per C<sub>60</sub> to  $\sim 4.5$  electrons per C<sub>60</sub>. We observe a maximum  $T_c$  of 52 K for 3–3.5 holes per C<sub>60</sub>, which is almost five times higher than for electron-doping in the same geometry (11 K)<sup>13</sup> and is to the best of our knowledge the highest  $T_c$  reported for a non-copper-oxide superconductor. We also analyse the dependence of the superconductivity on the charge carrier density induced by gate-doping.

## Sample preparation

We prepared FETs on C<sub>60</sub> crystals grown by physical vapour transport<sup>18</sup>. This transport process is an efficient method of purifying C<sub>60</sub>. A charge of 10 to 20 mg C<sub>60</sub> (pre-purified by multiple sublimations) was placed in a quartz tube (both sides open) inside a horizontal furnace and was exposed to a stream of pure hydrogen, flowing at a rate of 40–100 ml min<sup>−1</sup> at a temperature of 600 °C. Crystals 1–2 mm in size nucleated spontaneously on the reactor

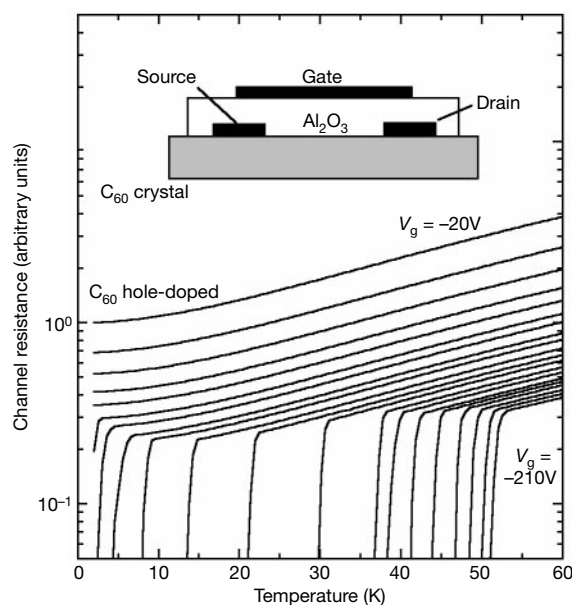


**Figure 1** Channel resistance of a C<sub>60</sub> single-crystal field-effect transistor. The gate voltage ( $V_g$ ) was varied between  $-20$  and  $-210$  V in  $-10$  V increments; the shift of the transition temperature  $T_c$ , indicated by the break in the slope, with the applied bias is clearly observable. Inset, the field-effect transistor geometry used in the experiments.

wall, and grew stress free to the centre of the reactor. These crystals have faces that are either (100) or (111); we removed these crystals from the reactor and deposited (by evaporation) gold source and drain electrodes, forming a channel of  $\sim 25\ \mu\text{m}$  length and  $500\text{--}1,000\ \mu\text{m}$  width. An aluminium oxide dielectric layer and a gate electrode complete the FET structure (see Fig. 1 inset). These devices show n- as well as p-channel activity, reflecting the ambipolar transport in these high-quality single crystals and further emphasizing the low interface state density of the FETs<sup>13</sup>. The electrical measurements were performed in a Quantum Design system by sweeping either the temperature ( $T$ ) or the gate voltage ( $T > 1.7\ \text{K}$ , magnetic field up to  $9\ \text{T}$ ).

Using the field-effect doping technique, we have demonstrated superconductivity in electron-doped  $\text{C}_{60}$  single crystals at  $11\ \text{K}$  (ref. 13). Moreover, we have used this technique to create a metallic state in organic molecular crystals, such as pentacene, tetracene and anthracene<sup>14</sup>. These materials were the first hydrocarbon superconductors<sup>14</sup>.

### Hole superconductivity

Figure 1 shows the channel resistance as a function of temperature for various negative gate voltages (hole-doping). The resistance systematically decreases as more holes are injected. The decrease is essentially linear in applied voltage, with a small offset at low voltages that might be associated with the presence of localized electronic states. The normal-state resistivities are in the range of a few  $\text{m}\Omega\ \text{cm}$ , assuming that the injected charge is confined to a single  $\text{C}_{60}$  molecular layer. The central result of this study is the observation of superconductivity above  $50\ \text{K}$  ( $T_c \approx 52\ \text{K}$ ).

In Fig. 2 we plot  $T_c$ —which is inferred from the breaks in the slope of the resistivity data—for two different samples versus the number of holes per molecule. The latter is calculated from the independently measured capacitance of the gate dielectric, assuming that all the charge is located in a single layer of molecules. This assumption is meaningful in the light of existing knowledge about FET structures and actual calculations for organic semiconductors<sup>19</sup>.

In addition to the high  $T_c$ , we also note that superconductivity occurs over a rather wide range of hole concentrations. Furthermore,  $T_c$  gradually increases after having reached the experimental lower limit of  $1.7\ \text{K}$  near 1 hole per  $\text{C}_{60}$ , and reaches a maximum between 3 and 3.5 holes per  $\text{C}_{60}$ . Over the limited range of data from this study, the initial rise of  $T_c$  appears to be gradual, suggesting an exponential or power-law dependence (see Fig. 2 inset). Therefore, following  $T_c$  to lower concentrations and temperatures, where other

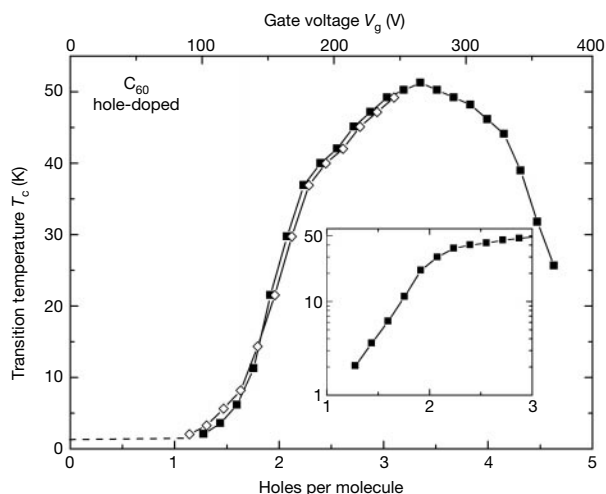


**Figure 2** Transition temperature  $T_c$  as a function of hole density for two samples.  $T_c$  exhibits a maximum of  $52\ \text{K}$  at approximately 3.2 holes per  $\text{C}_{60}$ . The minimum measurable  $T_c$  in the experimental set-up ( $1.7\ \text{K}$ ) is indicated by the dashed line. Inset, data replotted on a semi-logarithmic scale.

many-body ground states might occur, is desirable. The continuous increase of  $T_c$  with increasing hole concentration appears to be in contrast to the sharp onset of gate-induced superconductivity in hole-doped polyacene single crystals<sup>12</sup>. At the highest doping level ( $\sim 4.5$  holes per  $\text{C}_{60}$ ),  $T_c$  drops to half its maximum value. The two sets of  $T_c$  values from different samples are in good agreement, and both suggest a shoulder in the  $T_c$  curve near 2–2.5 holes per  $\text{C}_{60}$ , which corresponds to a quarter-filled valence band. Further studies will be needed in order to determine if this feature reflects a structure in the density of states.

The superconducting coherence length  $\xi$ , one of the characteristic parameters of superconductivity, can be deduced from the suppression of  $T_c$  in a magnetic field  $H$ . In Fig. 3 we plot  $T_c(H)$  with the field applied perpendicular to the superconducting layer for a carrier concentration that results in a  $T_c$  of  $41.5\ \text{K}$ . The slope of the upper critical field  $dH_{c2}/dT$  is  $\sim 0.7\ \text{T K}^{-1}$  and the usual extrapolation yields  $20\ \text{T}$  for  $H_{c2}$  at  $T = 0$ . This corresponds to a coherence length of  $40\ \text{\AA}$ , which is similar to the values measured in electron-doped  $\text{C}_{60}$  (refs 1–3).

### $T_c$ versus carrier concentration

In the following discussion of additional data, we try to shed some light on the origin of the high  $T_c$  in hole-doped  $\text{C}_{60}$ . It is helpful to keep in mind that  $T_c$  can be varied experimentally by changing the band filling (doping level) or by changing the bandwidth (lattice parameter). We will first discuss our FET data, which are results for a fixed lattice parameter ( $\sim 14.16\ \text{\AA}$ ) and bandwidth. We will then discuss the effect of lattice-parameter variation in  $\text{A}_3\text{C}_{60}$ ; this variation resulted from the insertion of ions (A) of various size by chemical doping.

In Fig. 4a we compare the dependence of  $T_c$  on the density of electrons and holes, and we find significant differences. We induced up to almost 5 electrons per  $\text{C}_{60}$ , and thereby mapped out the dependence of  $T_c$  (above  $1.7\ \text{K}$ ) on the electron density. Previous data on chemically doped bulk samples have shown a very similar peaking of  $T_c$  near 3 electrons per  $\text{C}_{60}$  (ref. 20), and thus the superconducting region extends from  $\sim 2.5$  to 3.6 electrons per  $\text{C}_{60}$ , close to half-filling of the LUMO band. In the case of hole-doping  $T_c$  is almost five times higher and, moreover, the superconductivity range is much wider. Furthermore,  $T_c$  reaches its maximum of  $52\ \text{K}$  at 3–3.5 holes per  $\text{C}_{60}$ , less than the 5 holes per  $\text{C}_{60}$  which would correspond to half filling of the HOMO bands. At 5 holes per  $\text{C}_{60}$ ,  $T_c$  either vanishes or is at least strongly suppressed.

The results in Fig. 4 represent an extremely wide shift of the chemical potential through the electronic states of a solid, corresponding to a continuous variation from a ‘half-empty’ valence band to a ‘half-filled’ conduction band. It is thus tempting to compare  $T_c$  to the underlying electronic DOS. Figure 4b shows

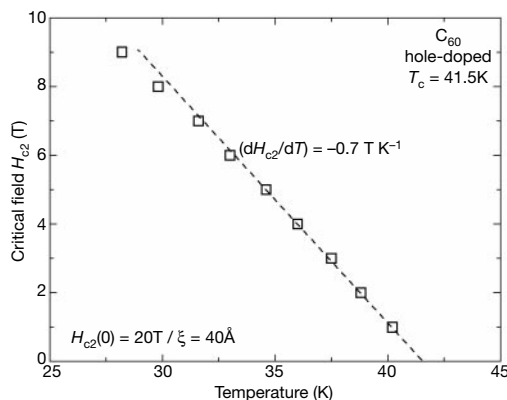


**Figure 3** Critical magnetic field  $H_{c2}$  as a function of temperature. A superconducting coherence length  $\xi_0$  of  $40\ \text{\AA}$  and an upper critical field  $H_{c2}(0)$  of  $20\ \text{T}$  can be estimated from the temperature dependence of  $H_{c2}$ .

the DOS calculated for  $C_{60}$  (ref. 6), as a function of induced charge per molecule rather than as a function of energy. This calculation was done for a bulk three-dimensional solid. Our situation is different in that the two-dimensional (2D) metal is sandwiched between the undoped  $C_{60}$  bulk and the aluminium oxide gate dielectric. Although it would be highly desirable to repeat the calculations for the present situation, we will simply assume that the essential features of the DOS in Fig. 4b remain relevant.

First, we notice that the DOS on the hole-doping side is indeed greater than on the electron-doping side, as expected for the higher degeneracy of the states. Second,  $T_c$  does not bear a close resemblance to the DOS curve. The maxima in  $T_c$  occur at doping levels well removed from the DOS maxima. This is particularly noticeable on the hole-doping side, where the DOS peaks strongly near 1 hole per  $C_{60}$ , while  $T_c$  is below the experimental threshold of 1.7 K. Third, a significant carrier density has to be introduced before superconductivity is observed (above 1.7 K), well after the metallic state is developed, as indicated by the temperature dependence of the resistivity. Further detailed studies of the resistivity near  $T_c$  are required to investigate the importance of 2D fluctuations in the gate-induced 2D superconductors. Homogeneous doping by chemical means appears not to be possible for this range<sup>12</sup>. Thus, Fig. 4 reveals that the DOS might not be the dominant factor determining  $T_c$ , and that  $T_c$  is also strongly modified by a filling-dependent coupling strength. This is not unexpected considering that the bands are derived from three and five molecular orbitals, respectively. For the doping range explored here, more than one sub-band is occupied by holes and electrons. The coupling strengths for these sub-bands are obviously not the same.

### Coupling strength

Insight into the coupling strength can be gained by examining the resistivity above  $T_c$ . Figure 5 shows the resistivity  $\rho(T)$  for electron and hole doping, with the hole concentration chosen to produce a  $T_c$  similar to the maximum  $T_c$  for electron doping, that is, approximately 1.8 holes per  $C_{60}$  compared to 3 electrons per  $C_{60}$  (see Fig. 4).

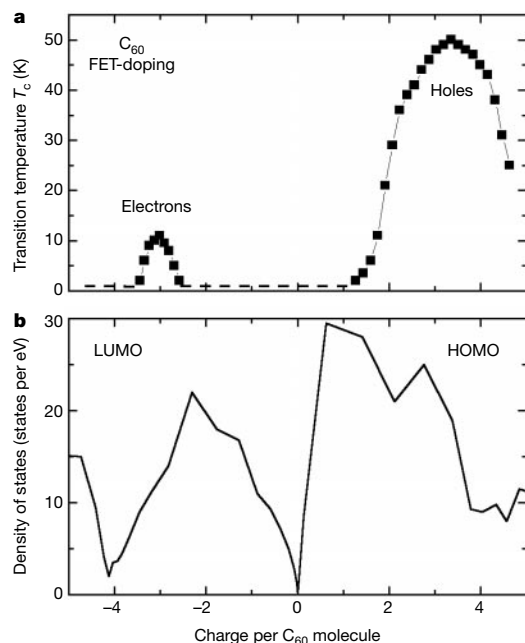


**Figure 4** Transition temperature and density of states as a function of charge per  $C_{60}$  molecule. **a**, The transition temperature for electron-doped and hole-doped  $C_{60}$  in the present FET geometry. In these gate-doped devices, the maximum  $T_c$  is 11 K for electrons and 52 K for holes. The broken line indicates the doping range where no superconductivity above 1.7 K was found in this study. **b**, The electronic density of states calculated for three-dimensional bulk  $C_{60}$  (ref. 5).

For a quantitative comparison, the measured  $\rho(T)$  for the hole-doped metal has been multiplied by a factor 1.8/3 in order to account for the difference in carrier density (both curves are for 3 charge carriers per molecule and can, therefore, also be compared to  $A_3C_{60}$ ). This linear scaling with carrier concentration is indeed appropriate, as we have found in extensive studies of  $\rho(T)$  for various carrier concentrations in this range, which will be discussed elsewhere.

The main result in Fig. 5 is clear: the resistivity of the hole-doped metal is five to six times higher than that of the electron-doped metal, for the same number of charge carriers per molecule. This difference indicates stronger hole-phonon than electron-phonon coupling, and thus the difference in  $T_c$  has to be ascribed to differences in coupling strength. We now consider some features of the  $\rho(T)$  curves in Fig. 5. Both data sets reflect the phase transition near 250 K (ref. 21) in the form of an approximately 5% reduction in  $\rho(T)$ . The absolute resistivity values of the FET electron-doped  $C_{60}$  can be compared with those of chemically doped  $C_{60}$ , either in bulk or in thin-film form<sup>1,22</sup>. The residual resistivity  $\rho_0$  in the present samples is in the range 250–300  $\mu\Omega$  cm, and is thus about half that of very good chemically doped  $A_3C_{60}$  samples. However, the temperature-dependent part of the resistivity  $\rho(T) - \rho_0$  is significantly larger in the gate-doped samples, resulting in a variation of  $\rho(T) - \rho_0$  from  $\leq 20 \mu\Omega$  cm at  $T_c$  to  $\sim 1.8 \text{ m}\Omega$  cm at room temperature<sup>23</sup> (see Fig. 6). This variation is only  $\sim 0.5 \text{ m}\Omega$  cm in chemically doped  $C_{60}$ .

The hole-doped metal is different from the electron-doped metal not only in terms of the coupling strength, which is in accordance with theoretical estimations<sup>10</sup>, but also in the details of the coupling. This is shown in Fig. 6, where we plot  $\rho(T) - \rho_0$  on a logarithmic scale. (Keeping in mind that the measured data are not corrected for possible temperature-induced differential strains and for thermal expansion effects<sup>24,25</sup>, a comparison is nevertheless meaningful since all experimental parameters are the same for the two curves, except for the sign of the applied gate voltage.) At low temperatures the resistivity of the electron-doped metal varies less rapidly than that of the hole-doped metal. At higher temperatures, however, both types vary in a similar way:  $\rho \propto T^n$  with  $n \approx 2$ . (This is expected from scattering of electron or holes in two dimensions by acoustic phonons in a three-dimensional crystal; C. M. Varma, personal communication.) The two metallic states therefore differ also in the energy dependence of the coupling constant, the hole-doped metal

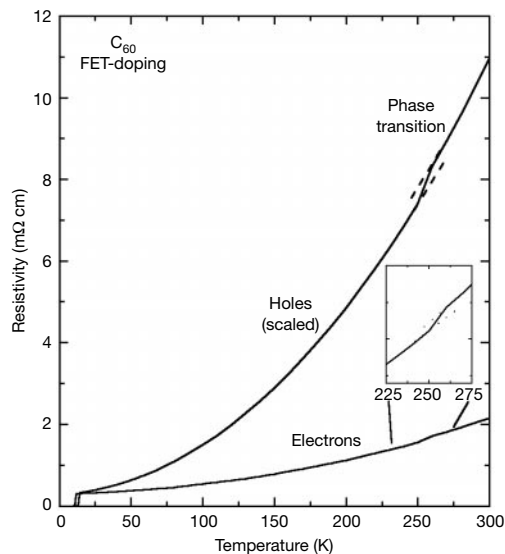


**Figure 5** Resistivity of electron- and hole-doped  $C_{60}$  as a function of temperature. The resistivity of the hole-doped sample has been scaled (multiplied by  $\sim 0.6$ ) in order to compare samples of the same carrier density (three charge carriers per molecule). The superconducting phase transition at low temperatures and the structural phase transition around 255 K are clearly observable.

having more weight at low energies. As the resistivity is given by the DOS at the Fermi level,  $N(0)$ , times the square of the coupling strength,  $\lambda^2$ , we cannot extract the values of  $\lambda$  independently. If the hole DOS is about twice the electron DOS, as can be estimated for the three-dimensional case, the ratio of the  $\lambda$  values is approximately 1.5, which is reasonable in the light of the  $T_c$  ratio. The experimental approach employed here offers an opportunity for future detailed studies of the coupling strength and its temperature (and energy) dependence as the chemical potential is moved through the band structure.

### Outlook

The  $T_c$  value of 52 K for hole-doped  $C_{60}$  is to our knowledge the highest yet reported for a non-copper-oxide superconductor. Furthermore, the lattice parameter  $a_0$  in the FET geometry is essentially that of undoped  $C_{60}$  crystals ( $a_0 \approx 14.16 \text{ \AA}$ ). It has been demonstrated<sup>1-3</sup> that  $T_c$  can be substantially raised by expanding the lattice through incorporation of ions. In the present geometry, where the metallic layer is clamped, the gate-induced charge might slightly modify the intramolecular bond lengths. It is

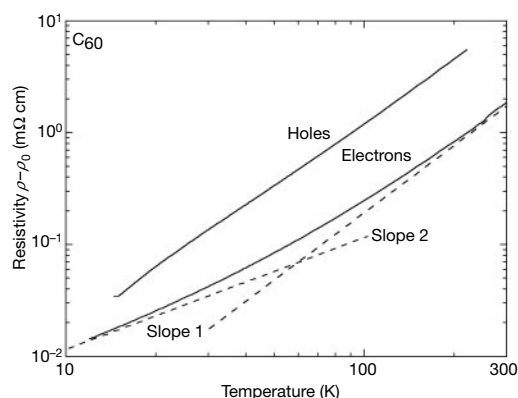


**Figure 6** Difference of the resistivity  $\rho$  and the residual resistivity  $\rho_0$  as a function of temperature. The dashed lines show a power-law dependence with exponent one and two for comparison.

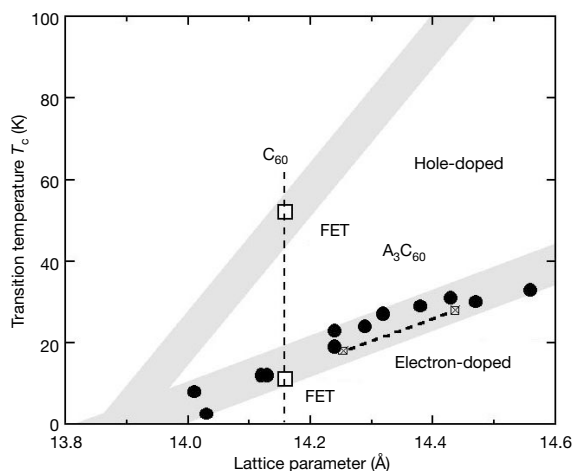


**Figure 7** Transition temperature in electron- and hole-doped  $C_{60}$  as function of lattice parameter. In  $A_3C_{60}$ , with three electrons per  $C_{60}$ , the lattice parameter is varied through the size of the inserted A ion (Na, K, Rb, Cs)<sup>1-3</sup> and extrapolates to a very small value for lattice parameters in the range of 13.8–13.9 Å (filled circles, lower grey line). The dotted line represents the  $T_c$  variation when the lattice parameter is reduced by hydrostatic pressure<sup>1-3</sup>. The lower open square shows  $T_c$  when three electrons, as in  $A_3C_{60}$ , are introduced in  $C_{60}$  crystals through the gate voltage in a field-effect geometry (FET)<sup>12</sup>. The upper open square is the present result for FET hole-doped  $C_{60}$ . Assuming similar scaling of  $T_c$  in hole- and in electron-doped  $C_{60}$ , the upper grey line is an attempt to extrapolate  $T_c$  for hole-doped  $C_{60}$  with an expanded lattice.

unclear to what extent the intermolecular distances and therefore the electronic bandwidth would be affected by this. However, this effect will be significantly smaller than the variation of the intermolecular distances due to the insertion of ions or neutral molecules by chemical doping for a fixed carrier density (see Fig. 7). This observation has been ascribed<sup>1-3</sup> to the change of bandwidth (that is, DOS) due to variations of the wavefunction overlap between adjacent molecules.

The effect of alkali-metal doping is well studied for  $A_3C_{60}$ , and amounts to an increase of  $T_c$  from  $\sim 14$ –15 K at  $a_0 \approx 14.16 \text{ \AA}$  to  $T_c \approx 33$  K for  $a_0 \approx 14.56 \text{ \AA}$  (refs 1–3). To estimate the influence of a similar lattice expansion for the hole-doped situation we attempt a semi-quantitative estimation of  $T_c$  (Fig. 7). Underlying this estimation is the experimental result for  $A_3C_{60}$  that  $T_c$  extrapolates to zero for a lattice parameter of 13.9 Å, owing to the rapid broadening of the LUMO band leading to a decrease of the DOS. This band broadening will also hold for the HOMO states and, therefore, one might, in a simplified way, draw a straight line between this point and the experimental value of 52 K as an extrapolation of  $T_c$ . If lattice expansions similar to those achieved in the past for electron-doping could be realized also with hole-doped  $C_{60}$ , we anticipate that values of  $T_c$  well above 100 K could be achieved (for  $a_0 \approx 14.6 \text{ \AA}$ ). □

Received 5 September; accepted 30 October 2000.

- Seitz, F. & Turnbull, D. *Solid State Physics* Vol. 48 (eds Ehrenreich, H. & Spaepen, F.) (Academic, San Diego, 1994).
- Ramirez, A. P.  $C_{60}$  and its superconductivity. *Supercond. Rev.* **1**, 1–101 (1994).
- Gunnarsson, O. Superconductivity in fullerenes. *Rev. Mod. Phys.* **69**, 575–606 (1997).
- Hebard, A. F. *et al.* Superconductivity at 18 K in potassium-doped  $C_{60}$ . *Nature* **350**, 600–601 (1991).
- Varma, C. M., Zaanen, J. & Raghavachari, K. Superconductivity in the fullerenes. *Science* **254**, 989–992 (1991).
- Erwin, S. C. in *Buckminsterfullerenes* (eds Billups, W. E. & Ciufolini, M. A.) 217–255 (VCH, New York, 1992).
- Haddon, R. C., Siegrist, T., Fleming, R. M., Bridenbaugh, P. M. & Laudise, R. A. Band structures of organic thin-film transistor materials. *J. Mater. Chem.* **5**, 1719–1724 (1995).
- Mazin, I. I. *et al.* Quantitative theory of superconductivity in doped  $C_{60}$ . *Phys. Rev. B* **45**, 5114–5117 (1992).
- Hirsch, J. E. Bond-charge repulsion and hole superconductivity. *Physica C* **158**, 326–336 (1989).
- Haddon, R. C. The fullerenes: powerful carbon-based electron acceptors. *Phil. Trans. R. Soc. Lond. A* **343**, 53–62 (1993).
- Reed, C. A., Kim, K. C., Bolskar, R. D. & Mueller, L. J. Taming superacids: stabilization of the fullerene cations  $HC_{60}^+$  and  $C_{60}^+$ . *Science* **289**, 101–104 (2000).
- Song, L. W., Fredette, K. T., Chung, D. D. L. & Kao, Y. H. Superconductivity in interhalogen-doped fullerenes. *Solid State Commun.* **87**, 387–391 (1993).
- Schön, J. H., Kloc, Ch., Haddon, R. C. & Batlogg, B. A superconducting field-effect switch. *Science* **288**, 656–658 (2000).
- Schön, J. H., Kloc, Ch. & Batlogg, B. Superconductivity in molecular crystals induced by charge injection. *Nature* **406**, 704–706 (2000).
- Kochanski, G. P., Hebard, A. F., Haddon, R. C. & Fiory, A. T. Electrical resistivity and stoichiometry of  $K_3C_{60}$  films. *Science* **255**, 184–186 (1992).
- Rosseinsky, M. J. Recent developments in the chemistry and physics of metal fullerenes. *Chem. Mater.* **10**, 2665–2685 (1998).
- Han, J. E., Koch, E. & Gunnarsson, O. Metal-insulator transitions: influence of lattice structure, Jahn-Teller effect, and Hund's Rule coupling. *Phys. Rev. Lett.* **84**, 1276–1279 (2000).
- Kloc, Ch., Simpkins, P. G., Siegrist, T. & Laudise, R. A. Physical vapor growth of centimeter-sized crystals of  $\alpha$ -hexathiophene. *J. Cryst. Growth* **182**, 416–427 (1997).
- Dodabalapur, A., Torsi, L. & Katz, H. E. Organic transistors: two-dimensional transport and improved electrical characteristics. *Science* **268**, 270–271 (1995).
- Yildirim, T. *et al.*  $T_c$  vs. carrier concentration in cubic fullerene superconductors. *Phys. Rev. Lett.* **77**, 167–170 (1996).
- Heiney, P. A. *et al.* Discontinuous volume change at the orientational-ordering transition in solid  $C_{60}$ . *Phys. Rev. B* **45**, 4544–4547 (1992).
- Hesper, R., Tjeng, L. H., Heeres, A. & Sawatzky, G. A. BCS-like density of states in superconducting  $A_3C_{60}$  surfaces. *Phys. Rev. Lett.* **85**, 1970–1973 (2000).
- Klein, O., Grüner, G., Huang, S.-M., Wiley, J. B. & Kaner, R. B. Electrical resistivity of  $K_3C_{60}$ . *Phys. Rev. B* **46**, 11247–11249 (1992).
- Crespi, V. H., Hou, J. G., Xiang, X.-D., Cohen, M. L. & Zettl, A. Electron-scattering mechanisms in single-crystal  $K_3C_{60}$ . *Phys. Rev. B* **46**, 12064–12067 (1992).
- Vareka, W. A. & Zettl, A. Linear temperature dependent resistivity at constant volume in  $Rb_3C_{60}$ . *Phys. Rev. Lett.* **72**, 4121–4124 (1994).

### Acknowledgements

We thank E. A. Chandross and C. M. Varma for discussions, and E. Bucher for the use of his equipment.

Correspondence and requests for materials should be addressed to B.B (e-mail: batlogg@lucent.com).



## Superconductivity at 52 K in hole-doped C<sub>60</sub>

J. H. Schön, Ch. Kloc & B. Batlogg

*Nature* **408**, 549–552 (2000).

This manuscript was, in part, the subject of an independent investigation<sup>1</sup> conducted at the behest of Bell Laboratories, Lucent Technologies. The independent committee reviewed concerns related to the validity of data associated with the device measurements described in the paper. As a result of the committee's findings, we are issuing a retraction of the paper. We note nevertheless that this paper may also contain some legitimate ideas and contributions. □

1. Beasley, M. R., Datta, S., Kogelnik, H., Kroemer, H. & Monroe, D. Report of the Investigation Committee on the Possibility of Scientific Misconduct in the Work of Hendrik Schön and Coauthors. (<http://publish.aps.org/reports/>) (doi:10.1103/aps.reports.lucent) (Lucent Technologies/American Physical Society, September 2002).

## Superconductivity in molecular crystals induced by charge injection

J. H. Schön, Ch. Kloc & B. Batlogg

*Nature* **406**, 702–704 (2000).

Several papers were recently the subject of an independent investigation<sup>1</sup> conducted at the behest of Bell Laboratories, Lucent Technologies. The independent committee reviewed concerns related to the validity of data associated with the device measurements described in those papers. As a result of the committee's findings, we have issued retractions of those papers. Furthermore, because of the extensive and serious nature of the committee's findings relating to the manuscripts that they examined, we are additionally concerned

about aspects of the data presented in this paper. As we cannot vouch for the validity of the data, we wish to withdraw our support for the paper and issue a retraction.

The first author of this paper (J.H.S.), who was responsible for most of the experimental work, wishes to be dissociated from this retraction because he believes in the science presented in this manuscript. □

1. Beasley, M. R., Datta, S., Kogelnik, H., Kroemer, H. & Monroe, D. Report of the Investigation Committee on the Possibility of Scientific Misconduct in the Work of Hendrik Schön and Coauthors. (<http://publish.aps.org/reports/>) (doi:10.1103/aps.reports.lucent) (Lucent Technologies/American Physical Society, September 2002).

## Efficient organic photovoltaic diodes based on doped pentacene

J. H. Schön, Ch. Kloc, E. Bucher & B. Batlogg

*Nature* **403**, 408–410 (2000).

Several papers were recently the subject of an independent investigation<sup>1</sup> conducted at the behest of Bell Laboratories, Lucent Technologies. The independent committee reviewed concerns related to the validity of data associated with the device measurements described in those papers. As a result of the committee's findings, we have issued retractions of those papers. Furthermore, because of the extensive and serious nature of the committee's findings relating to the manuscripts that they examined, we are additionally concerned about aspects of the data presented in this paper. As we cannot vouch for the validity of the data, we wish to withdraw our support for the paper and issue a retraction.

The first author of this paper (J.H.S.), who was responsible for most of the experimental work, wishes to be dissociated from this retraction because he believes in the science presented in this manuscript. □

1. Beasley, M. R., Datta, S., Kogelnik, H., Kroemer, H. & Monroe, D. Report of the Investigation Committee on the Possibility of Scientific Misconduct in the Work of Hendrik Schön and Coauthors. (<http://publish.aps.org/reports/>) (doi:10.1103/aps.reports.lucent) (Lucent Technologies/American Physical Society, September 2002).